

Toughness of glass fibres reinforced glass-ionomer cements

P. LUCKSANASOMBOOL^{*,§}, W. A. J. HIGGS^{‡,§}, R. J. E. D. HIGGS^{*,‡},
M. V. SWAIN^{‡,§,¶,**,†}

^{*}Faculty of Medicine, [‡]Department of Mechanical & Mechatronic Engineering,

[§]Biomaterials Science Research Unit, Faculty of Dentistry, University of Sydney

E-mail: mswain@mail.usyd.edu.au

Two fracture toughness parameters, the critical stress intensity factor, K_c and the work of fracture, W_f have been used to characterise the toughness of conventional and resin-modified glass-ionomer cements reinforced with glass fibres. The critical stress intensity factor was determined from the peak load, and the work of fracture was determined as the energy required to extend an introduced crack through the respective glass ionomers. For both materials, crack propagation became more stable as the weight fraction of glass fibres was increased. Additionally, when the weight percent of glass fibres was increased the work of fracture increased. Fibre bridging at the crack tip resulted in the increase in the work of fracture. As the percentage weight of fibres was increased, the critical stress intensity factor decreased proportionally to the increase in porosity.

© 2002 Kluwer Academic Publishers

1. Introduction

The problem with the adhesion of dental restorative materials to dental tissues led to the development of polyelectrolyte cements. Not only do these materials have the ability to bond to enamel and dentine, but they also possess good physical properties and low toxicity. However, these zinc and other metal oxide based polyelectrolyte cements are opaque and unaesthetic [1]. Glass-ionomer cements (GICs) developed by Wilson and co-workers during the late 1960's were a major breakthrough in the development of acceptable dental restorative materials [2]. These materials possess a significant number of attractive features including the release of fluoride to enhance caries resistance [3], good biocompatibility [4, 5], aesthetics, and they also adhere well to dental tissues [6]. GICs are currently used in dentistry for many clinical applications such as luting agents and restorative materials. In addition, glass ionomer cements have shown their potential in other medical areas, such as orthopaedic surgery [7, 8]. However, because their mechanical properties are relatively poor, attempts have been made in the endeavour to improve their properties by such means as; modification of the composition (glass and liquid compositions) [9–16], resin-modified GICs [17–19], and reinforced GICs (metal or fibres) [20–26].

The mechanical properties of the conventional GICs change markedly with modification in the glass powder

composition, the liquid component, and the powder/liquid ratio. Unfortunately, changes in the mechanical properties are not as significant as changes in the handling properties that result from these modifications [9–16].

The mechanical properties of resin-modified GICs have been shown to be superior to those of conventional GICs [27–29]. The weak organic-salt matrix of conventional GICs is strengthened by the cross-linked polymerisation of introduced resin systems [1]. However, the fracture toughness of these resin-modified GICs are still lower than those of the acrylic bone cements {Poly(methylmethacrylate), PMMA} [27, 28, 30]. Increases in the strength and fracture toughness of these types of cements (GICs & PMMA) by the method of fibre reinforcement have been reported previously [23, 26, 31, 32].

The aim of this study was to investigate whether fibre reinforcement would lead to improvements in the toughness of a conventional GIC (Fuji I) and an experimental resin-modified GIC (S-430). The experimental resin-modified GIC (S-430) was developed by modifying the conventional GIC with hydroxyethylmethacrylate (HEMA) monomer (Table I). The toughness parameters investigated were the critical stress intensity factor (K_c), which characterises the stress distribution at the crack tip, and the work of fracture (W_f), which represents the energy required to create new fracture surfaces.

[¶]Author to whom all correspondence should be addressed.

^{**}Present Address: Biomaterials Science Research Unit, Suite G11, National Innovation Centre, Australian Technology Park, Eveleigh, NSW 1430, Australia.

TABLE I Compositions of materials used

Materials	Powder	Particle size	Liquid	Consistency	P/L ratio
FUJI I	Fluoro-alumino-silicate glass 95% Powdered poly(acrylic acid) 5%	Less than 15 μm	Polybasic carboxylic acid (10% Conc.) 50% Water 50%	Low	1.8 g/1.0 g
S-430	Fluoro-alumino-silicate glass 100%	Less than 15 μm	Poly(acrylic acid) 30% HEMA 30% Methylmethacrylate 10% Water 30%	Low	1.8 g/1.0 g

2. Materials and methods

The glass fibres used in this study were manufactured by a proprietary process and were supplied by the GC Corporation, Japan. The glass fibres have the same composition as glass powder used in glass ionomer cement supplied by the company. The fibres were supplied in a chopped format and had various diameters ranging from 20 to 100 μm , and aspect ratios ranging from 10–20 (Fig. 1). Glass fibres were added to the base powders of each material in the following proportions: 0, 10, 20, and 30% by weight. The fibre and powder composition was then mixed manually with the corresponding poly(acrylic acid) liquid component at a powder/liquid ratio (P/L) of 1.8. The resultant cement paste was placed into a Teflon single edged notch beam fracture toughness mould, dimensioned according to (ASTM E399-83 [33]). The mould was subsequently pressurised, and the cement was allowed to set at room temperature (22.5°C). After 15 minutes, the

specimens were removed from the mould and stored in physiologically buffered saline (PBS). The specimens were polished and notched using a low speed diamond saw. The specimens were stored in PBS at 37°C for 1 week prior to mechanical testing.

Mechanical testing was conducted in 3-point bending mode (single edge notched bending test) using a Shimadzu Materials Testing Machine. The specimens were tested in a PBS bath at room temperature at a crosshead rate of 0.25 mm s^{-1} . The fracture toughness, K_{c} , was calculated from the critical load, P_{Q} , using the following relationship:

$$K_{\text{c}} = \frac{P_{\text{Q}}S}{BW^{\frac{3}{2}}} f(a/W)$$

where S is the support span, B is the specimen breadth, and $f(a/W)$ is a dimensionless function of a/W , namely

$$f(a/W) = \frac{3(a/W)^{\frac{1}{2}}[1.99 - (a/W)(1 - a/W) \times (2.15 - 3.93a/W + 2.7a^2/W^2)]}{2(1 + 2a/W)(1 - a/W)^{\frac{3}{2}}}$$

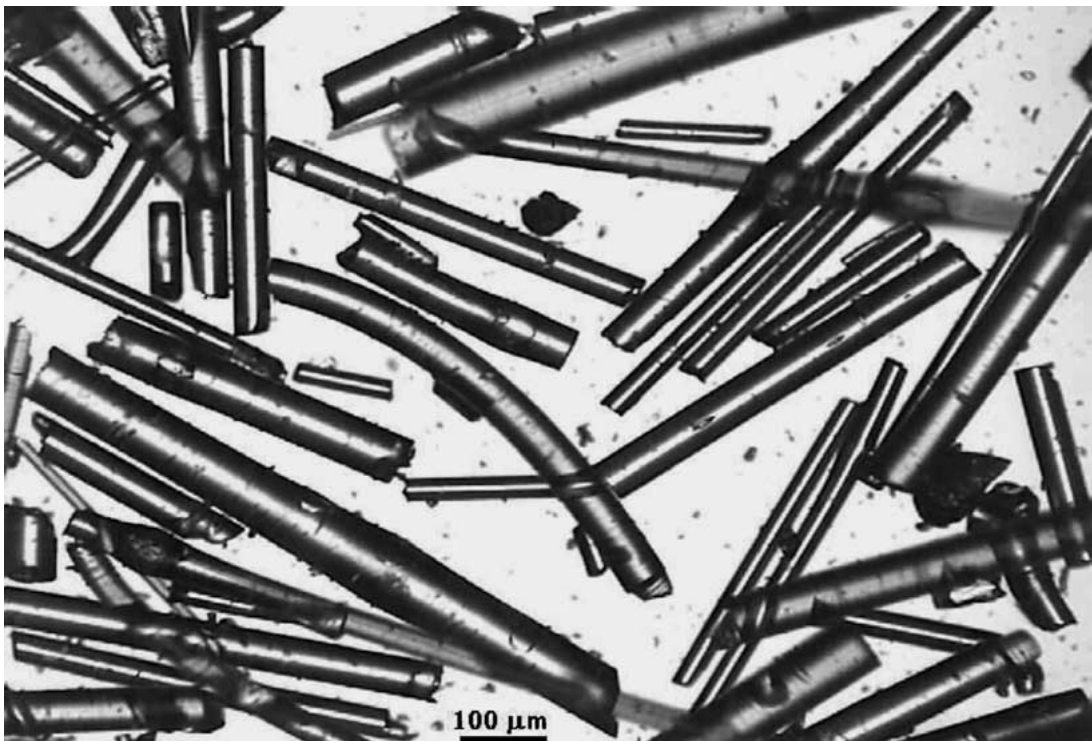


Figure 1 Experimental glass fibres manufactured by GC Corporation with diameters ranging from 20 to 100 μm and a typical aspect ratio of 10–20.

The work of fracture, W_f , or the energy per unit area of new fracture surface, was calculated from the area under the load/displacement curve divided by the fracture surface area. The critical strain energy release rate, G_c , was calculated from K_c by the relationship:

$$G_c = \frac{K_c^2(1 - \nu^2)}{E_c}$$

where E_c is the apparent flexural modulus of the cement and ν is poisson's ratio.

Observation of the fracture surfaces was performed using a scanning electron microscope (SEM). A Carbon coating was applied to the fracture surfaces of the specimens to minimize electrostatic charging.

3. Results

Figs 2 and 3 show the average load/displacement curves for each group of specimens containing glass fibres i.e. 0, 10, 20, 30% by weight. The load/displacement curves for all specimens showed an initial elastic portion, but different 'yielding' behaviour. The specimens without fibres (0%) showed the highest stiffness whereas the specimens with the highest percent fibre (30%) showed

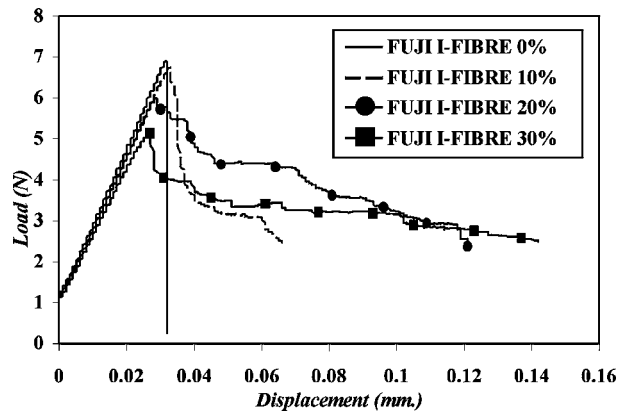


Figure 2 The load/displacement curves of conventional GIC (FUJI I) with glass fibres, 0%, 10%, 20%, and 30% by weight. The stiffness changes only with 30% glass fibres, while the area under the curves increase as the percent weight of glass fibres increase.

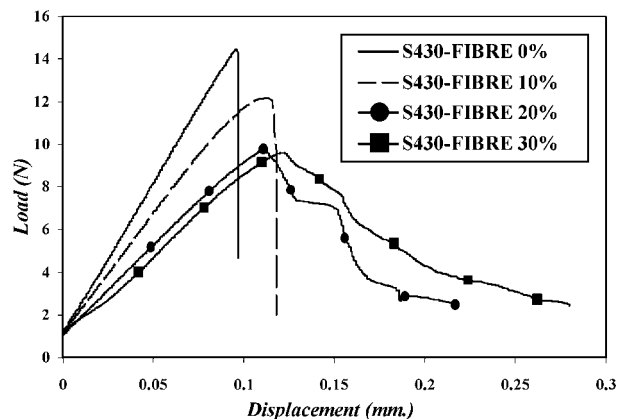


Figure 3 The load/displacement curves of resin-modified GIC (S-430) with glass fibres, 0%, 10%, 20%, and 30% by weight. The stiffness decreases and the area under the curves increase as the percent weight of glass fibres increase.

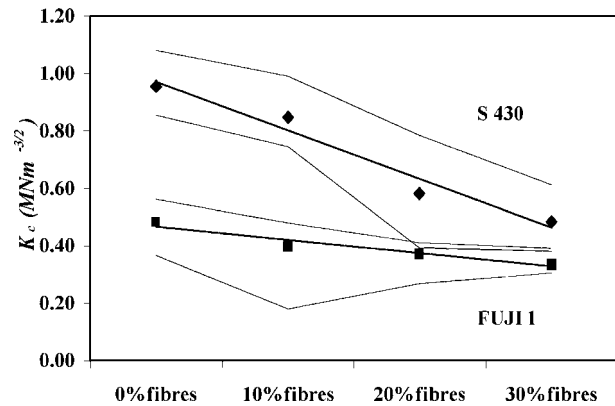


Figure 4 Maximum, average, and minimum values of K_c of GICs with glass fibres 0%, 10%, 20%, and 30% by weight, K_c decreases as the percent weight of glass fibres increase.

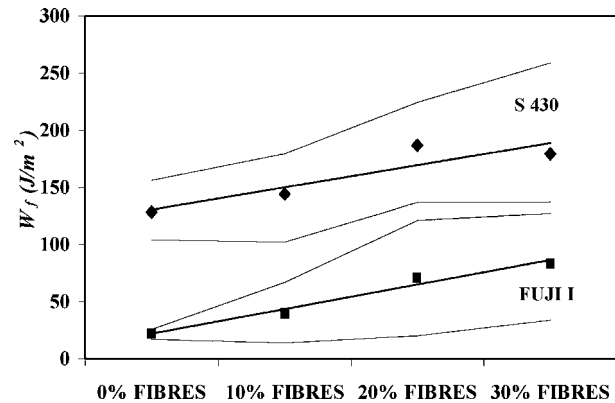


Figure 5 Maximum, average, and minimum values of W_f of GICs with glass fibres 0%, 10%, 20%, and 30% by weight, W_f increases as the percent weight of glass fibres increase.

the lowest stiffness. The most striking difference between the specimens that contained fibres was their post 'yielding' behaviour. The specimens without fibres failed in a catastrophic manner, whilst the specimens that contained fibres developed a broad yield-like response; exhibiting stable crack propagation. The area under the load/displacement curve, which corresponds to the energy required to propagate the crack, increased as the weight percent of the glass fibres increased.

Figs 4 and 5 show average values of the critical stress intensity factor and the work of fracture for each group respectively. The critical stress intensity factor decreased as the percent of glass fibres increased. The work of fracture, by contrast, increased as the percent of glass fibres increased. The apparent flexural moduli for both the conventional and resin-modified GICs, calculated from the slope of the load/displacement curve, decreased as the percent of glass fibres increased (Fig. 6). Fig. 7 illustrates the increase in the energy of fracture as the percent of glass fibres is increased for both material systems. Prior to fracture, the resin-modified GIC shows a greater component of energy absorption when compared with the conventional GIC.

Fig. 8 provides an illustrative comparison of the fracture surfaces of both the conventional and resin-modified GICs. Of particular interest is the noticeable increase in the level of porosity as the weight percent of glass fibres is increased. More notable is the level

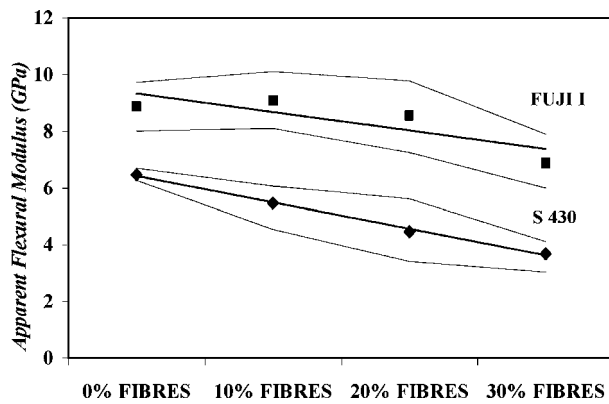


Figure 6 Maximum, average, and minimum values of the apparent flexural moduli, E_c , of GICs with glass fibres 0%, 10%, 20%, and 30% by weight calculated from the stiffness of the load/displacement curves. E_c decreases as the percent weight of glass fibres increase.

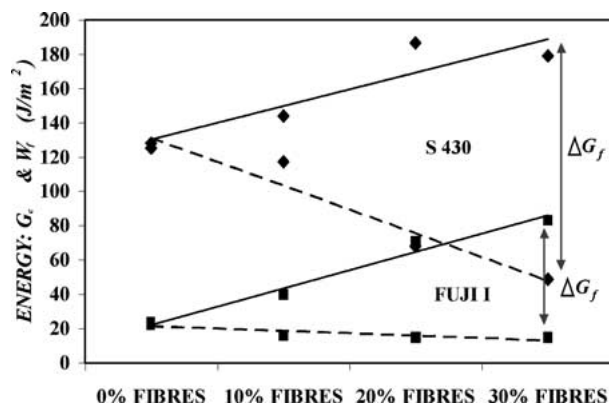


Figure 7 Comparison of W_f and calculated G_c shows an increase of toughness (ΔG_f) as the percent weight of glass fibres increase.

of porosity in the resin-modified GIC at the 30% fibre level. Figs 9 and 10 reveal fracture surfaces of conventional and resin-modified GICs with 30% fibres. Both figures illustrate the random orientation of the glass fibres, the characteristic fibre pull-out mechanism, and ubiquitous cracking through the cement matrix.

4. Discussion

The results for the critical stress intensity factor from this study confirm that the magnitudes reported for the conventional GIC (Fuji I) without fibre reinforcement ($0.48 \pm 0.06 \text{ MNm}^{-3/2}$) is within the range of data previously reported ($0.3\text{--}0.5 \text{ MNm}^{-3/2}$) [28, 34–37]. However, generally, commercially different GICs have distinct glass and liquid {poly(acrylic acid)} components, which lead to a difference in fracture toughness magnitudes [11–16]. Differences in toughness can be attributed to different modes of testing and/or testing conditions [36, 38, 39]. Fujishima and Ferracane [39], for instance, demonstrated this fact by examining four different testing methods to establish a single value for fracture toughness. They found large variation in toughness parameters for each test. Consistently, different specimen geometries develop different crack front profiles, which in turn lead to differences in the calculation of the critical stress intensity factor [36]. Mitchell *et al.* [38] demonstrated that hydration of GICs after expo-

sure to air, cause an inherent scatter in toughness data. Experiments conducted in dry condition [35, 36] reveal lower fracture toughness values when compared to experiments conducted in physiological conditions [34]. This effect is attributed to an increase in the number of pre-existing cracks in the dry or dehydrated state [38].

A large variation also exists in the strength of resin-modified GICs. Their strengths depend, to a large extent, on the type of resin component [27]. The critical stress intensity factor of resin-modified GIC without fibre reinforcement used in this study ($0.96 \pm 0.08 \text{ MNm}^{-3/2}$) was also within the range of the values previously reported (0.30 ± 0.07 to $1.37 \pm 0.10 \text{ MNm}^{-3/2}$) for resin-modified GIC systems [27, 28]. The failure characteristic presented from the load/displacement curves [Figs 2 and 3 (0% fibres)], revealed brittle-like behaviour of both systems.

In this study, the addition of fibres to both the conventional and the resin-modified GICs changed the traditional mode of fracture from brittle to a more ductile type failure [40]. Generally, the fibre-modified cements exhibit more stable crack extension (Figs 2 and 3). The existence of this yielding type behaviour indicates the presence of a toughening mechanism. The toughening mechanism appears to be predominantly facilitated by the bridging of fibres across the extending crack. The SEM images confirm the existence of breaking and pull-out of the fibres (Figs 9 and 10). The observations match theoretical predictions for chopped-fibre cementitious materials. For these materials, the addition of fibres to brittle matrices neither increases the initial cracking stress (the critical stress intensity factor) nor generally improves the ultimate composite strength [41]. The main purpose of fibre-reinforcement is to control the cracking process [41], by providing closure bridging forces across the extending crack thereby reducing the stress intensity at the crack tip and improving the toughness [42]. In this study, the critical stress intensity factor for crack initiation decreased as the weight percent of the glass fibres increased. This can be explained by the increase in the porosity of the cement as the weight percent of the fibres increases (Fig. 8) resulting in a lower stiffness as shown by the reduced slope of the initial loading curve, which can be represented as the apparent flexural modulus (Fig. 6 and Table II) and greater ease of crack initiation. However, with an increase of glass fibre content, the extent of bridging forces also increases resulting in greater crack stability and the increase in the work of fracture. That is, the materials exhibit increasing fracture resistance with crack extension or R-curve type behaviour.

Micromechanical analysis of the fibre-reinforced composite theoretically relies on each of the following key elements, the volume fraction of fibre (V_f), matrix (V_m), and void (V_v) [43]. In addition to the volume fraction, the property and size of the fibre, the type of matrix, and the interfacial characteristics between the fibre and matrix contribute to the overall mechanical properties of the fibre-reinforced composite [44]. The fracture toughness of fibre-reinforced materials, G_t , may be written as:

$$G_t = G_0 + \Delta G_f$$

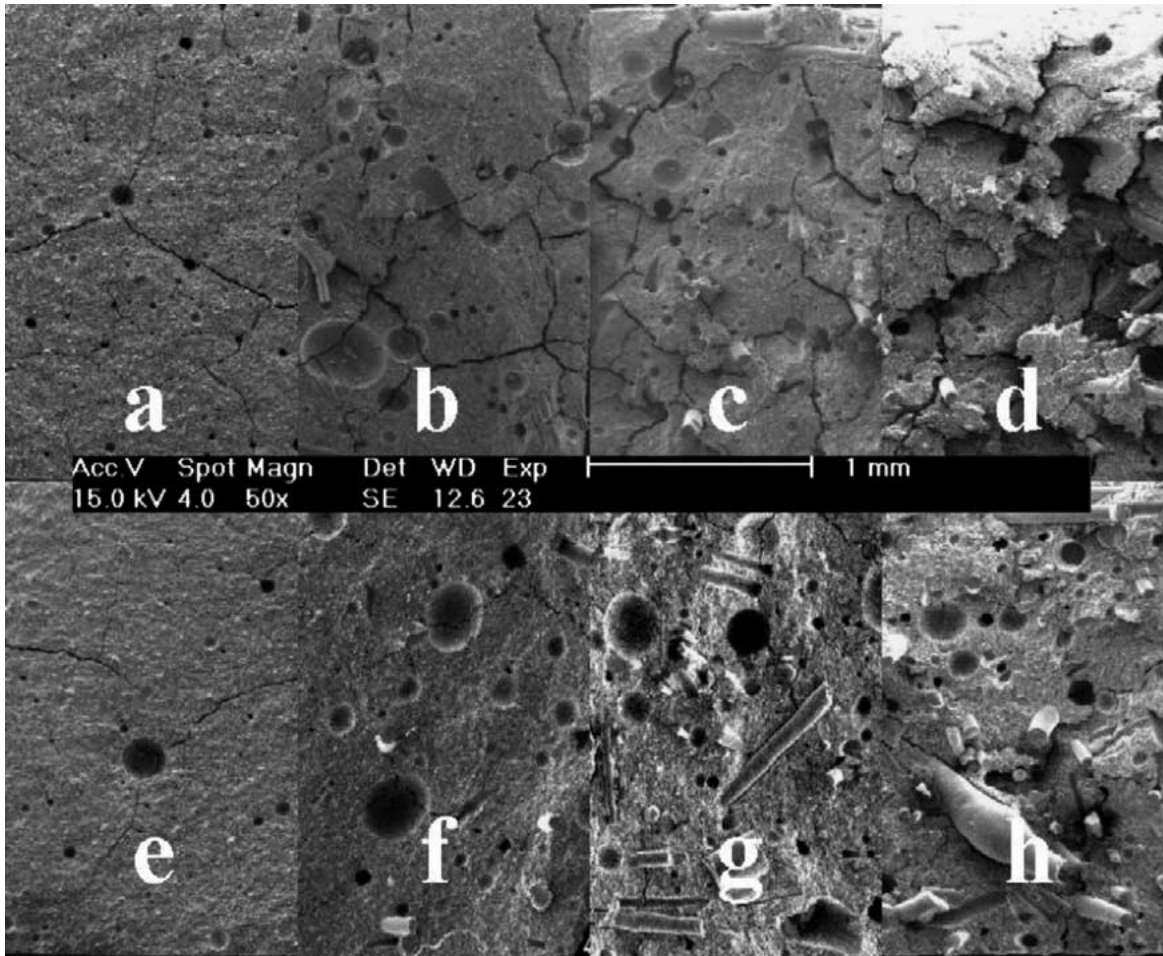


Figure 8 SEM image of the fracture surfaces shows an increase of porosity as the percent weight of glass fibres increase (a to d for FUJI I and e to h for S-430). Resin-modified GICs (S-430) show higher degree of porosity than conventional GIC (FUJI I).

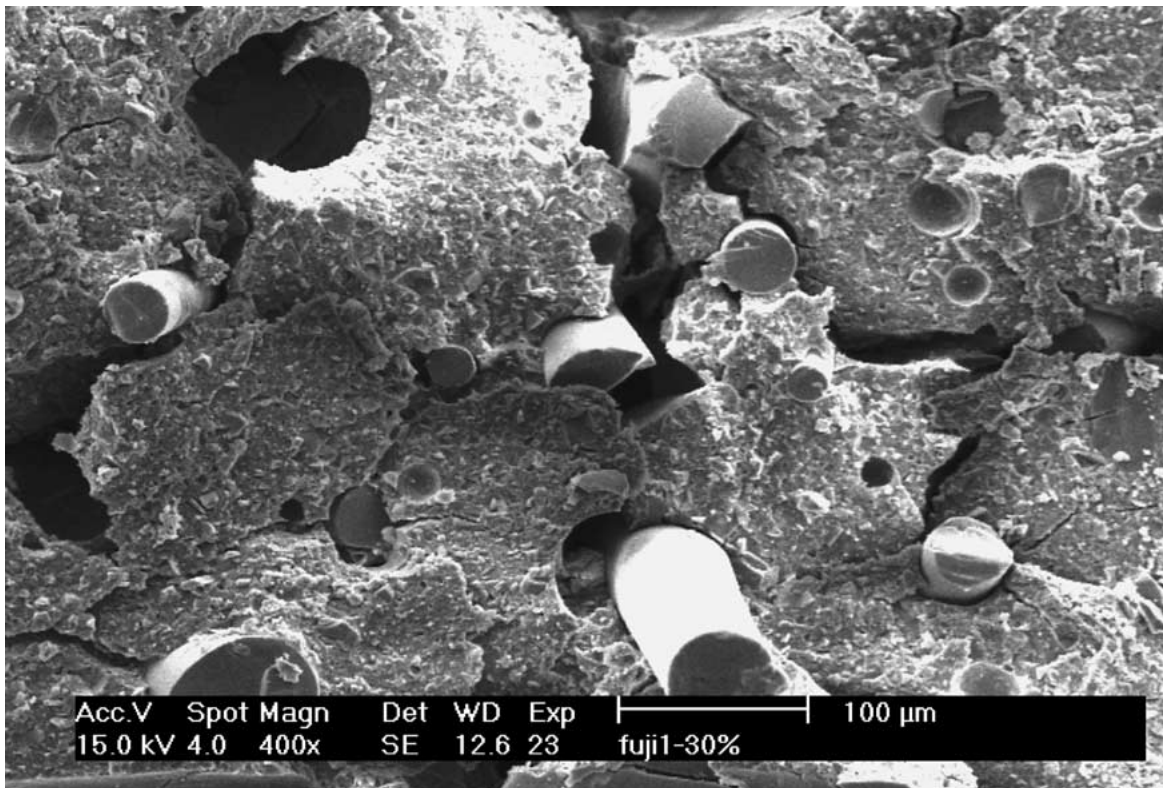


Figure 9 Higher magnification of FUJI I fracture surface demonstrates random orientation of the glass fibres, pull-out fibres, and cracks through the cement matrix.

TABLE II K_c , W_f , and E_c of GICs as the weight percent of glass fibres increase

	0% Fibres	10% Fibres	20% Fibres	30% Fibres
		Stress intensity factor (K_c)($\text{MNm}^{-3/2}$)		
FUJI I	0.48 ± 0.06	0.40 ± 0.09	0.37 ± 0.04	0.34 ± 0.03
S 430	0.96 ± 0.08	0.85 ± 0.08	0.58 ± 0.12	0.48 ± 0.07
		Work of fracture (K_f)(J/m^2)		
FUJI I	22.16 ± 3.47	40.05 ± 16.24	70.92 ± 35.53	83.24 ± 35.56
S 430	128.12 ± 18.87	144.03 ± 25.47	186.54 ± 29.74	179.00 ± 38.60
		Apparent flexural modulus (E_c)(GPa)		
FUJI I	8.86 ± 0.86	9.21 ± 0.90	8.02 ± 0.78	7.20 ± 0.70
S 430	6.47 ± 0.21	5.84 ± 0.19	5.44 ± 0.18	3.95 ± 0.13

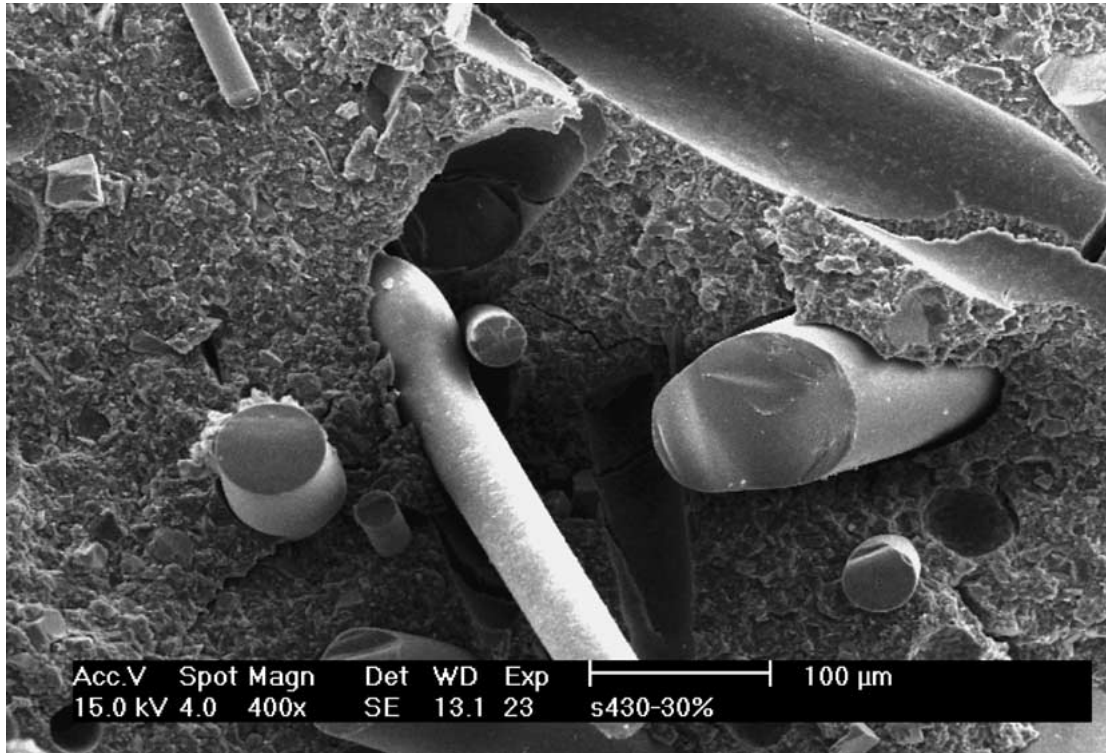


Figure 10 Higher magnification of S-430 fracture surface demonstrates random orientation of the glass fibres, pull-out fibres, and cracks through the cement matrix.

where G_0 is the toughness of the matrix and ΔG_f is the toughness increment of the fibres [45]. The toughness increases because of crack face bridging or closure forces, and is given by:

$$\Delta G_f = 2 \int_0^{u^*} \rho(u) du$$

where $\rho(u) = V_f \sigma(u)$, V_f is the volume fraction of fibres, and $\sigma(u)$ is the closure stress of a bridging element. From both systems (conventional and resin-modified GICs), the toughening effect of glass fibres in the brittle matrix increases linearly as the weight percent of glass fibres increase (Fig. 7). The addition of glass fibres is an efficient toughening mechanism, increasing the toughness of the conventional GIC from 22 to 83 J/m^2 with 30% fibre and from 128 to 179 J/m^2 for the resin-modified material. The toughening effect is significantly higher for the resin-modified material suggesting that the pull-out force is higher presumably because of the better bonding of the poly-HEMA to the glass fibres. This assumption seems reasonable because

even in the absence of fibres, there is a higher increase in the toughness and strength of the resin-modified GIC. Addition of the same amount of glass fibres to the resin-modified GIC shows more effective toughening than to the conventional GIC. This effect reflects the different interfacial characteristics of the two systems. The final set structure of the conventional GIC is presented as a complex composite of glass particles surrounding by a siliceous hydrogel and bonded together by a matrix phase consisting of hydrated fluoridated calcium and aluminum polyacrylates, while that of resin-modified GIC has the conventional GIC entangled with poly(hydroxyethyl methacrylate) hydrogel as an interpenetrating polymer network [1]. The bonding ability of the poly-HEMA to both the glass fibres and particles, as well as the poly(acrylic acid) network, results in a different interfacial bonding ability. The role of the matrix/fibre interface is of great importance. The adhesion must not be too strong that the fibres rupture prematurely before debonding can ensue; nor must it be too weak that the frictional resistance to sliding is reduced [45]). A previous review by McCabe [29] has

indicated that the bonding ability of a resin-modified GIC to enamel and dentine is greater than that of a conventional GIC. Hence, the toughening effect of glass fibres may also be enhanced by improving the interfacial bond between the fibres and matrix as in the case of resin-modified GIC.

Another feature that we have not included in this study, is the effect of the type and size of the fibres. Kobayashi *et al.* [26] demonstrated the effects of different types and sizes of glass fibres on the strengths of reinforced GICs. The smaller diameter and shorter fibres result in higher diametral tensile strengths (DTS). Additionally, the use of such smaller fibres may also be expected to improve the toughening effect of these glass fibres. However, as pointed out by an anonymous reviewer, both this work and that of Kobayashi *et al.* [26] failed to consider the effect of powder to liquid ratio upon replacing high surface area powder by lower reactive fibres. This effect will certainly reduce the number of Al⁺ ions available to assist with the cross linking of the poly(acrylic acid). This may partially account for the decreasing strength and modulus of the fibre-reinforced cements.

As the present observations indicate, the improvement of the glass ionomer cements' toughness (the work of fracture) can be achieved by the addition of fibres and the toughness increased as the weight percent of the fibres increased. However, there were some limitations mainly due to the influence of the fibres on matrix properties and the interfacial bonding. Of particular concern is that it affects the handling properties and flow properties of the cement which has been also mentioned by Topoleski *et al.* [32]. Theoretically, addition of any type of fibre should increase the steady state fracture toughness of a fibre-reinforced material. However, to achieve a steady state value, considerable crack extension must occur so that the crack bridging mechanism is established behind the extending crack tip. Practically, handling of the cement with fibres is more difficult and results in the increase of porosity of the cement. The development of mixing and handling techniques, such as centrifugation [32], are as significant as the development of the cement properties.

5. Conclusions

The present study has clearly identified a number of significant effects associated with the reinforcement of GICs with glass fibres of the same composition as the glass particulate matrix. They are:

1. Fracture stability increases with increasing volume fraction of glass fibres.
2. A decrease in the critical stress intensity for crack initiation with increase of glass fibres. This appeared to be related to the increased porosity with glass fibre content.
3. The work of fracture increased linearly with increase in volume fraction of fibres with more than a two-fold increase in this volume with 30% of fibres.
4. The toughening increment associated with fibres increased linearly with volume fraction of fibres.

5. The GIC containing HEMA was significantly greater than toughening increment for the conventional GIC.

Acknowledgments

W.A.J. Higgs acknowledges a scholarship support and supply of materials from the GC Corporation. Dr. N. Suansuwan is thanked for taking the SEM pictures in this study.

References

1. D. C. SMITH, *Biomaterials* **19** (1998) 467.
2. A. D. WILSON and B. E. KENT, *Journal of Applied Chemistry and Biotechnology* **21** (1971) 313.
3. M. ROTHWELL, H. M. ANSTICE and G. J. PEARSON, *Journal of Dentistry* **26** (1998) 591.
4. P. J. DOHERTY, *Clinical Materials* **7** (1991) 335.
5. A. OLIVA, R. F. DELLA, A. SALERNO, V. RICCIO, G. TARTARO, A. COZZOLINO, S. D'AMATO, G. PONTONI and V. ZAPPIA, *Biomaterials* **17** (1996) 1351.
6. J. W. McLEAN and A. D. WILSON, *British Dental Journal* **136** (1974) 269.
7. L. M. JONCK, C. J. GROBBELAAR and H. STRATING, *Clinical Materials* **4** (1989) 201.
8. L. M. JONCK and C. J. GROBBELAAR, *ibid.* **6** (1990) 323.
9. S. CRISP, B. G. LEWIS and A. D. WILSON, *Journal of Dentistry* **4** (1976) 287.
10. *Idem.*, *ibid.* **5** (1977) 51.
11. E. DE BARRA and R. G. HILL, *Biomaterials* **19** (1998) 495.
12. S. GRIFFIN and R. G. HILL, *J. Mater. Sci.* **33** (1998) 5383.
13. S. G. GRIFFIN and R. G. HILL, *Biomaterials* **20** (1999) 1579.
14. *Idem.*, *ibid.* **21** (2000) 399.
15. E. DE BARRA and R. G. HILL, *ibid.* **21** (2000) 563.
16. S. G. GRIFFIN and R. G. HILL, *ibid.* **21** (2000) 693.
17. A. D. WILSON, *International Journal of Prosthodontics* **3** (1990) 425.
18. Y. MOMOI, K. HIROSAKI, A. KOHNO and J. F. McCABE, *Dental Materials Journal* **14** (1995) 109.
19. S. GLADYS, M. B. VAN, M. BRAEM, P. LAMBRECHTS and G. VANHERLE, *Journal of Dental Research* **76** (1997) 883.
20. A. W. WALLS, J. ADAMSON, J. F. McCABE and J. J. MURRAY, *Dental Materials* **3** (1987) 113.
21. J. J. SIMMONS, *Journal of the American Dental Association* **120** (1990) 49.
22. R. E. KERBY and R. F. BLEIHOLDER, *Journal of Dental Research* **70** (1991) 1358.
23. C. W. B. OLDFIELD and B. ELLIS, *Clinical Materials* **7** (1991) 313.
24. K. H. CHUNG, *Journal of Oral Rehabilitation* **20** (1993) 79.
25. N. K. SARKAR, *Dental Materials* **15** (1999) 421.
26. M. KOBAYASHI, M. KON, K. MIYAI and K. ASAOKA, *Biomaterials* **21** (2000) 2051.
27. R. E. KOVARIK and M. V. MUNCY, *American Journal of Dentistry* **8** (1995) 145.
28. C. A. MITCHELL, W. H. DOUGLAS and Y.-S. CHENG, *Dental Materials* **15** (1999) 7.
29. J. F. McCABE, *Biomaterials* **19** (1998) 521.
30. G. LEWIS, J. NYMAN and H. H. TRIEU, *ibid.* **19** (1998) 961.
31. J. L. GILBERT, D. S. NEY and E. P. LAUTENSCHLAGER, *ibid.* **16** (1995) 1043.
32. L. D. T. TOPOLESKI, P. DUCHEYNE and J. M. CUCKLER, *ibid.* **19** (1998) 1569.
33. ASTM Standards E399-83, in "American Society for Testing and Materials" (Philadelphia, PA, 1983).
34. M. GOLDMAN, *Journal of Biomedical Materials Research* **19** (1985) 771.
35. D. W. JACOBS, W. H. DOUGLAS, C. P. LIN and Y. S. L. CHENG, *Journal of Dental Research AADR* **74** (1995) 243.
36. M. W. BEATTY and R. M. PIDAPARTI, *Biomaterials* **14** (1993) 999.

37. R. M. PIDAPARTI and M. W. BEATTY, *Journal of Biomedical Materials Research* **29** (1995) 309.
38. C. A. MITCHELL, J. F. ORR and J. G. KENNEDY, *Biomaterials* **16** (1995) 11.
39. A. FUJISHIMA and J. L. FERRACANE, *Dental Materials* **12** (1996) 38.
40. S. POOLTHONG, T. MORI and M. V. SWAIN, *Dental Materials Journal* **13** (1994) 220.
41. A. M. BRANDT, "Cement-Based Composites: Materials, Mechanical Properties, and Performance" (E & FN Spon, London SE1 8HN, UK, 1995).
42. B. COTTERELL and Y. W. MAI, "Fracture Mechanics of Cementitious Materials" (Blackie Academic & Professional, Glasgow G64 2NZ, 1996).
43. R. F. GIBSON, "Principles of Composite Material Mechanics" (McGRAW-Hill, Singapore, 1994).
44. J. P. SCHAFFER, A. SAXENA, T. H. SANDERS JR. and S. B. WARNER, "The Science and Design of Engineering Materials" (Richard D. Irwin, INC., Chicago, 1995) p. 594.
45. B. LAWN, "Fracture of Brittle Solid" (Cambridge University Press, Melbourne 3166, Australia, 1993).

*Received 19 December 2000
and accepted 3 August 2001*